J. Biochem. 122, 627-634 (1997)

Identification of Two Nucleotide-Binding Domains on the PB1 Subunit of Influenza Virus RNA Polymerase[1]

Yukiyasu Asano*,† and Akira Ishihama*,[2]

Department of Molecular Genetics, National Institute of Genetics, Mishima, Shizuoka 411; and †Rational Drug Design Laboratories, Fukushima, Fukushima 960-12

Received for publication, April 30, 1997

Influenza virus RNA polymerase is a multifunctional and multisubunit enzyme consisting of three viral P proteins, PB1, PB2, and PA. We have previously shown that radioactive 8-azido GTP (8-N_3 GTP) was photo-crosslinked specifically to the PB1 subunit. Here we confirmed the specific crosslinking of PB1 using oxidized GTP and further identified the GTP analogue-binding domains after proteolytic cleavage of the crosslinked PB1 with V8 protease. The cleavage pattern of PB1 was determined by analysis of the amino-terminal proximal sequence of fragments generated in the presence of increasing concentrations of V8 protease. The GTP-crosslinking was identified in three fragments: two adjacent fragments, P6 starting from residue 179 and P11b starting from residue 298; and the third fragment, P11c, starting from residue 458. Thus, we propose that two GTP-binding sites exist in the PB1 subunit, *i.e.*, the amino terminal-proximal site I located at the boundary between P6 and P11b, and the carboxy terminal-proximal site II on P11c fragment. The locations of GTP-binding sites I and II are close to those of sequence motif A and motif D, respectively, conserved among RNA-dependent RNA polymerases. Of the two fragments forming site I, the crosslinking of 8-N_3 GTP is higher to P11b, while that of oxidized GTP is higher to P6, suggesting that the ribose and guanine moieties of GTP bound in this binding pocket face P6 and P11c, respectively. From the V8 concentration-dependent change in proteolytic cleavage pattern, it is likely that the two GTP-binding sites on PB1 protein are located on structurally different domains. The existence of two GTP-binding sites is discussed in relation to the binding sites for substrates, primers, and products.

Key words: cross-linking, influenza virus, RNA polymerase, substrate binding.

Influenza virus RNA-dependent RNA polymerase plays an essential role in both transcription and replication of the viral genome (*1-3*). For transcription, the RNA polymerase carries a number of activities, *i.e.*, recognition and binding of transcription promoters on viral RNA (vRNA), recognition and endonucleolytic cleavage of host-cell capped RNA molecules, capped RNA-primed initiation of RNA synthesis, RNA polymerization using nucleoside 5′-triphosphate substrates, binding of growing RNA chains, and addition of poly(A) tails to nascent mRNA. On the other hand, the same enzyme is involved in two-step reactions of replication, vRNA-directed synthesis of complementary RNA (cRNA) and cRNA-directed synthesis of vRNA. In replication, the RNA polymerase expresses different functions, *i.e.*, recognition of replication origins on both vRNA and cRNA templates, *de novo* initiation of RNA synthesis, and anti-termination of RNA chain elongation at poly(A) addition signal leading to the synthesis of template-sized RNA.

The viral RNA polymerase holoenzyme is composed of one molecule each of three viral encoded P proteins, PB1, PB2, and PA (*4*). Ultraviolet (UV) radiation-induced crosslinking studies indicated that PB2 is the cap 1-recognition protein (*5, 6*). In agreement with this prediction, temperature-sensitive (*ts*) mutants carrying mutant PB2 proteins exhibit defect in cap recognition as analyzed in capped RNA-primed RNA synthesis *in vitro* (*7*). These observations together suggest the involvement of PB2 in capped RNA recognition and cleavage. On the other hand, PB1 can be UV-crosslinked to substrates (*8*) and 3′-terminal nucleotides of elongating RNA chains (*9*), indicating that PB1 is the subunit involved in the catalytic activity of RNA polymerization. Since both PB1 and PB2 can be crosslinked to synthetic RNA with the 3′-terminal sequence of vRNA (*10*), these two basic subunits are considered to play roles in recognition of the transcription promoters and the replication origins. Even though no specific function has yet been identified for the PA protein, PA is considered to be involved in replication, because PA associates with PB1 to form a holoenzyme complex (*11*); *ts* mutant viruses carrying mutations in the PA gene are

[1] This work was supported by Grants-in-Aid from the Ministry of Education, Science, Sports and Culture of Japan, a research fund from the New Energy and Industrial Technology Development Organization (NEDO) of Japan, a CREST (Core Research for Evolutional Science and Technology) program of the Japan Science and Technology Corporation (JST) and a fund from the Rational Drug Design Laboratories.

[2] To whom correspondence should be addressed. Phone: +81-559-81-6741, FAX: +81-559-81-6746, E-mail, aishiham@lab.nig.ac.jp

Abbreviations: vRNA, viral RNA; cRNA, complementary RNA; 8-N_3 GTP, 8-azido GTP; RNP, ribonucleoprotein; DTT, dithiothreitol; PAGE, polyacrylamide gel electrophoresis; UV, ultraviolet.

defective in replication but not in transcription (*12, 13*); and the PB1-PB2 complex without PA is defective in the second step reaction, *i.e.*, cRNA-directed synthesis of vRNA, of replication *in vivo* (*14*).

To gain an insight into the functional role of each P protein and to make the functional map of each subunit polypeptide, we have performed a systematic analysis of mutant P proteins. We have determined the subunit-subunit contact sites for each P protein after analysis of complex formation in cells co-transfected with pairs of cDNA encoding one wild-type intact P protein and the other coding for deletion mutants of the second P protein (*11*). In parallel, we carried out crosslinking studies of substrates, capped RNA primers and model RNA templates to the P proteins. Recently, we have reported the affinity labeling of RNA polymerase PB1 subunit with 8-azido GTP (8-N_3 GTP), an azido analogue of GTP (*8*). Here, we confirmed this result by crosslinking experiments using an oxidized GTP with dialdehyde at the ribose moiety. In addition, we performed the domain mapping of PB1 protein by proteolytic cleavage and the identification of GTP-binding domains.

MATERIALS AND METHODS

Chemicals and Enzymes—8-Azido [α-^{32}P]GTP (8-N_3 GTP) (300 GBq/mmol) was purchased from ICN, USA. Dialdehyde [α-^{32}P]GTP was prepared by oxidation of [α-^{32}P]GTP (300 GBq/mmol) on ice for 2 h in the dark with 1 mM Na periodate in 0.5 mN HCl (*15*). Oxidation was terminated by adding two volumes of 50% glycerol. V8 protease was a product of Pierce (USA), while restriction enzymes were products of Takara (Otsu). All other chemicals used in this work were commercially available products of the highest quality.

Influenza virus A/PR/8/34 was used throughout this study. Viruses were grown in 10-day-old embryonated chicken eggs (a gift from Nippon Institute of Biological Science) at 34°C for 48 h, and purified by sucrose density gradient centrifugation as described previously (*8*). Ribonucleoprotein (RNP) cores were prepared from Nonidet P-40-treated virions as described (*4*).

Construction of PB1 Expression Plasmid—PB1 cDNA was isolated from pARP206 (*11*) after *Hin*dIII treatment (see the restriction enzyme map in Ref. *16*), treated with T4 DNA polymerase and inserted into pET3Sc by blunt-end ligation at *Sma*I site. pET3Sc is a modified version of pET3c, the expression plasmid under the control of T7 promoter/T7 RNA polymerase (*17*), by adding *Sma*I linker to the *Bam*HI site. The amino terminal-proximal sequence was modified so as to match the *Escherichia coli* codon usage pattern. In brief, a sequence of 526 nt in length downstream from the PB1 initiation codon of the PB1 gene was PCR-amplified using the following set of primers, GGCATATGGATGTCAATCGGACCTTACTTT-TCTTAAAAAGTG and CTCCATTACATCCTTAA, and pAPR206 as template. A promoter-proximal sequence of pET3ScPB1 between *Nde*I and *Afl*II including the T7 gene 10 protein and 5′-proximal sequence of the PB1 gene was replaced by the PCR product to make pETPB1M. The modified sequence was confirmed by DNA sequencing.

Purification of PB1 Protein—*E. coli* BL21(λDE3) transformed with pETPB1M was cultured in LB medium at 37°C. Expression of PB1 was induced by adding 0.1 mM isopropyl-β-D-thio-galactopyranoside (IPTG) and incubating for 3 h. Induced cells (about 3 g) were suspended in 30 ml of a lysis buffer consisting of 50 mM Tris-HCl (pH 7.5 at 4°C), 100 mM NaCl, 1 mM EDTA, 0.1 mM phenylmethylsulfonyl fluoride, 1% Nonidet P-40, and 1 mM dithiothreitol (DTT), and sonicated for five bursts, each consisting of 30 s pulse and 2 min pause, with a sonicator (model W- 225R Ultrasonics, USA). Cell lysates were centrifuged at 10,000 × *g* for 10 min. PB1 recovered in the pellet fraction was solubilized in a 0.1% SDS sample buffer containing 3% 2-mercaptoethanol and subjected to electrophoresis on 7.5% polyacrylamide gel (PAGE) in the presence of 0.1% SDS. Electrophoresis was performed for 4.5 h at a constant voltage of 150 V.

Photoaffinity Labeling of PB1 with 8-N_3 GTP—Photoaffinity labeling reaction was performed as described previously (*8*). In brief, the reaction mixture contained in a final volume of 20 μl (in a 1.5 ml conical tube): 50 mM Tris-HCl (pH 7.5 at 4°C), 1 mM $MgCl_2$, 25 μM 8-N_3 [α-^{32}P]GTP, and purified RNP (or purified virions plus 0.1% Nonidet P-40) containing about 0.1 μg of PB1 protein. After incubation at 30°C for 10 min in the dark, the mixture was exposed to irradiation at 254 nm UV for 3 min on ice with a Funa UV-Linker FS-1500 (Tokyo). Under the irradiation conditions employed, total irradiation energy was 1.0 J/cm^2. The samples were mixed with 2 μl of a quenching solution consisting of 100 mM EDTA and 200 mM DTT and after addition of 20 μl of 2% SDS-sample buffer, subjected to 7.5% PAGE in the presence of 0.1% SDS. Gels were stained with Coomassie Brilliant Blue R250.

Labeling of PB1 with Oxidized GTP—Isolated RNP including 0.1 μg PB1 protein was mixed with oxidized [α-^{32}P]GTP at 0°C in 50 mM Tris-HCl (pH 7.5), 5 mM $MgCl_2$, and 1 mM DTT. After addition of $NaCNBH_3$ at the final concentration of 5-10 mM, the cross-linking reaction was performed overnight at 0°C and terminated by adding TCA. TCA precipitates were analyzed by 7.5% PAGE in the presence of 0.1% SDS. Gels were stained with Coomassie Brilliant Blue R250.

V8 Protease Digestion of PB1 Protein and Analysis of Cleavage Products—The gel slice corresponding to the stained and ^{32}P-labeled PB1 band was cut out and soaked twice with 50 volumes of a gel soaking buffer [125 mM Tris-HCl (pH 6.8 at 30°C), 0.2% SDS, 1 mM EDTA, 10% glycerol, and 0.3% 2-mercaptoethanol] each for 2 h. In parallel, a gel slice containing about 10 μg of unlabeled PB1 was prepared using the PB1 protein expressed in *E. coli*. Both labeled and unlabeled gel slices were cut into five pieces, mixed and loaded into gel sample wells together with various concentrations of V8 protease in the gel sample buffer. Electrophoresis was performed in two steps: 8 h at 30 V for V8 digestion in 4% stacking gel; and 5 h at 120 V for peptide separation in 15% separation gel. Peptides were electrophoretically transferred onto an ProBlott transfer membrane (Applied Biosystems, USA). The membrane was stained with 0.025% Coomassie Brilliant Blue R250 in 40% methanol and 1% acetic acid, and destained with 40% methanol and 10% acetic acid. Radiolabeled peptides were detected by exposing the membrane to Kodak X-Omat AR film for autoradiography and was also analyzed with Bio-Image Analyzer (Fuji Film).

RESULTS

Identification of PB1 as the GTP-Binding Subunit—Crosslinking of 8-N_3 [α-^{32}P]GTP to influenza virus RNA polymerase was performed using both detergent-treated virions and isolated RNP cores. When purified virions were subjected to photo-induced crosslinking with 8-N_3 [α-^{32}P]-GTP, the radioactive nucleotide was crosslinked only to the PB1 subunit among viral structural proteins (*8*). Essentially the same result was obtained using isolated RNP cores (data not shown). Under the reaction conditions employed, the efficiency of photo-crosslinking was 1 to 5% of the PB1 protein present in the virions or RNP. To confirm the result, we also carried out the crosslinking experiment using oxidized [α-^{32}P]GTP with dialdehyde at its ribose moiety.

Periodate treatment of GTP leads to cleave the ribose moiety and the oxidized derivative of GTP can be crosslinked to exposed lysine on proteins *via* an unstable Schiff's base after reduction with cyanoborohydride (*15*). The result of crosslinking of influenza virus RNP with the oxidized GTP was essentially the same with that obtained with 8-N_3 [α-^{32}P]GTP (data not shown; see below for the binding site analysis), confirming that PB1 is the sole subunit crosslinked with GTP. These observations together support the concept that the catalytic site for RNA polymerization is located on the PB1 subunit. For identification of the GTP-binding site(s) on PB1, we performed proteolytic cleavage experiments.

Expression of the PB1 Protein in Escherichia coli—Since a large amount of PB1 protein was required for microsequencing of each proteolytic fragment derived from PB1, we first established the expression system of PB1 in *E. coli*. The complete cDNA for wild-type PB1 from influenza virus A/PR/8 was inserted into various expression vectors suitable for use in *E. coli*, but we failed to express the intact PB1 protein (data not shown). To overcome this difficulty, we prepared a modified version of the PB1 cDNA clone by changing the nucleotide sequence downstream from the translation initiation codon so as to match the *E. coli* codon usage pattern but without changing the amino acid sequence of PB1 protein (Fig. 1). Using this modified PB1 gene inserted into pET expression vector, the full-sized PB1 protein was successfully expressed at a detectable level and purified to homogeneity in sufficient quantity to carry out the proteolytic cleavage mapping. The amino-terminal proximal sequence of the expressed and purified PB1 protein was confirmed to be identical with the intact PB1 protein (data not shown). In addition to the intact PB1 protein, an additional band with the apparent M_r of 57,000 was identified after PAGE analysis of the induced cell extracts. The amino-terminal sequence analysis indicated

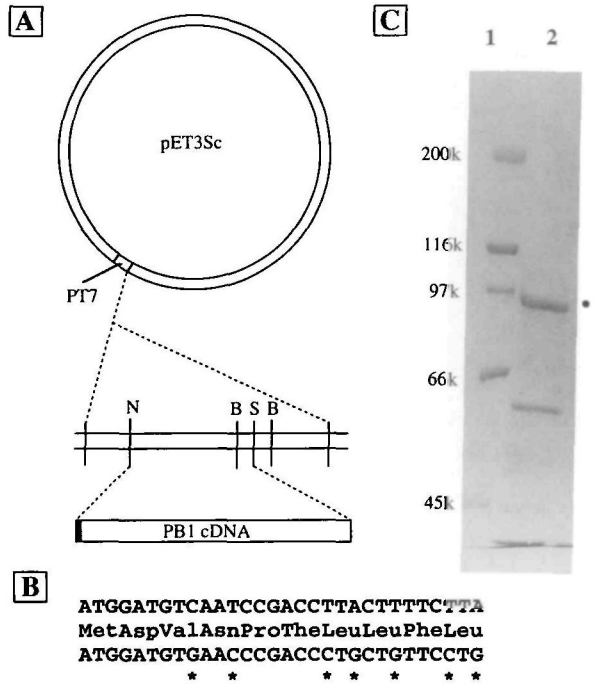

Fig. 1. **Construction of an *Escherichia coli* expression plasmid for PB1.** A: The nucleotide sequence of 5′-proximal region of cDNA for the PB1 gene of influenza virus A/PR8/34 was altered so as to match the *E. coli* codon usage but without changing the amino acid sequence. The modified cDNA was cloned into an *E. coli* expression vector pET3Sc to make pETPB1M. This plasmid expresses a non-fusion intact PB1 protein. Filled area on the PB1 cDNA indicates the region containing the modified nucleotide sequence. N, B, and S represent the sites for *Nde*I, *Bam*HI, and *Sma*I, respectively. B: The modified nucleotide sequence of cDNA for the PB1 protein. Upper lane, the original nucleotide sequence of the PB1 gene; middle lane, the amino acid sequence of amino-terminal proximal region of the PB1 protein; lower lane, the modified nucleotide sequence. The modified bases are indicated by stars. C: Expression of PB1 in *E. coli* using T7 promoter/RNA polymerase system. Expression plasmid, pETPB1M, was transformed into *E. coli* BL21(λ DE3). Expression of PB1 was induced by adding 0.1 mM IPTG. After 3 h culture at 37°C with shaking, cells were harvested and disrupted in 1% Nonidet P40. Cell lysate was centrifuged for 10 min at 10,000 × *g* and the pellet fraction (lane 2) was subjected to SDS-7.5% polyacrylamide gel electrophoresis. The protein size markers were run in parallel (lane 1). Dot indicates PB1 protein.

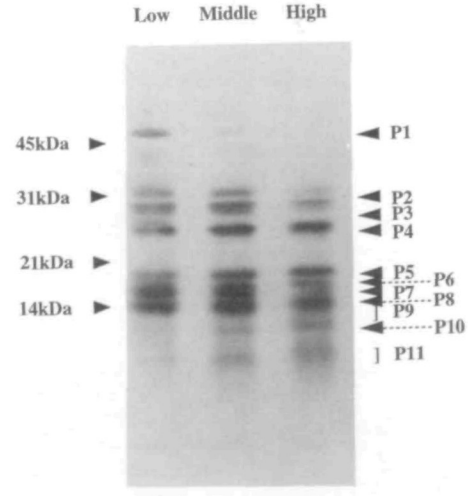

Fig. 2. **Isolation of V8 proteolytic fragments of the PB1 protein.** PB1 was expressed in *E. coli* and purified by SDS-PAGE. Purified PB1 was mixed with *Staphylococcus aureus* V8, subjected to 0.1% SDS-15% PAGE and digested in the stacking gel for 8 h at room temperature. The concentrations of V8 used were: low, 0.05 μg; middle, 0.5 μg; and high, 5 μg. After electrophoresis, proteolytic fragments were transferred onto a Pro-Blot PVDF membrane and stained with Coomassie Brilliant Blue R250. Migration positions of the marker proteins are indicated on the left side, while the PB1 fragments are marked on the right side.

that this protein is an amino terminal-truncated fragment of PB1 starting from Thr196. In agreement with this prediction, the proteolytic cleavage products of this 57 kDa protein by V8 protease are all included in the digestion products of intact PB1. From the level of accumulation, it was estimated that about half of the expressed PB1 protein was degraded by an as yet unidentified bacterial protease(s) at the boundary between the amino-terminal assembly domain with PB2 protein (*11*) and the internal functional domain for RNA synthesis.

The expression system for other two P proteins, PB2 and PA, was also established using the same strategy as employed for PB1 expression (data not shown). Preliminary experiments of the reconstitution of the RNA polymerase from individual subunits all expressed in *E. coli* indicated that the level of reconstitution of functional RNA polymerase remains at low levels, as in the case of reconstitution from P proteins expressed in the baculovirus-infected insect cells (*18*). In both cases, over-expressed P proteins formed inclusion bodies.

Determination of the Proteolytic Cleavage Order of PB1—Controlled cleavage of proteins by proteases is often employed for the mapping of structural and functional domains. Since PB1 expressed in *E. coli* formed insoluble aggregates, it was solubilized in a buffer containing 0.1% SDS. Even under the denatured conditions, some proteases such as V8 protease, chymotrypsin, and papain can be used for the cleavage mapping. Preliminary tests with these proteases indicated that the digestion by both chymotrypsin and papain is difficult to control, yielding a large number of small proteolytic fragments even at low protease concentrations or with short incubation times (data not shown). We thus decided to use V8 protease for the PB1 mapping.

PB1 was separated from *E. coli* proteins by SDS-PAGE and stained with Coomassie Blue R250. The PB1 gel band containing about 10 μg of PB1 was cut out, equilibrated with the sample buffer containing 0.1% SDS, mixed with different doses (0.05–5 μg per lane) of V8 protease, and subjected to the second cycle of SDS-PAGE. Proteolytic cleavage was carried out in the stacking gel and products were separated on 15% PAGE in the presence of 0.1% SDS. As shown in Fig. 2, at least 11 major bands were detected using three different doses of V8 protease, which are designated as P1 to P11 in decreasing order of molecular

TABLE I. **Amino-terminal sequences and sizes of V8 fragments of PB1.** V8 fragments were separated by SDS-PAGE and transferred onto Pro-Blot membranes. Amino-terminal sequence of each fragment was determined using Applied Biosystems 470A/900 protein sequencer. The sizes of V8 fragments were calculated from the mobility on SDS-PAGE.

Fragment	Size (kDa)	Amino acid sequence	N-terminal residue
P1	48.0	TMEVVQQTRV---	110
P2	30.3	TMEVVQQTRV---	110
P3	26.2	LSLTITGDNT---	298
P4	24.2	TMEVVQQTRV---	110
P5	17.8	SKSMKLRTQI---	359
P6	16.0	MGITTHFQRK---	179
P7a	15.0	MDVNPTLLFL---	1
P7b	15.0	IESMNNAVMM---	637
P8	13.6	SADMSIGVTV---	520
P9a	12.6	IESMNNAVMM---	637
P9b	12.6	YDAVATTHSW---	657
P10	11.5	SADMSIGVTV---	1
P11a		MDVNPTLLFL---	1
P11b		LSLTITGDNT---	298
P11c		GIQAGVDRFY---	458
P11d		DEQMYQRXXN---	685
PR1		TMEVVQQTRV---	110
PR2		SKSMKLRTQI---	359

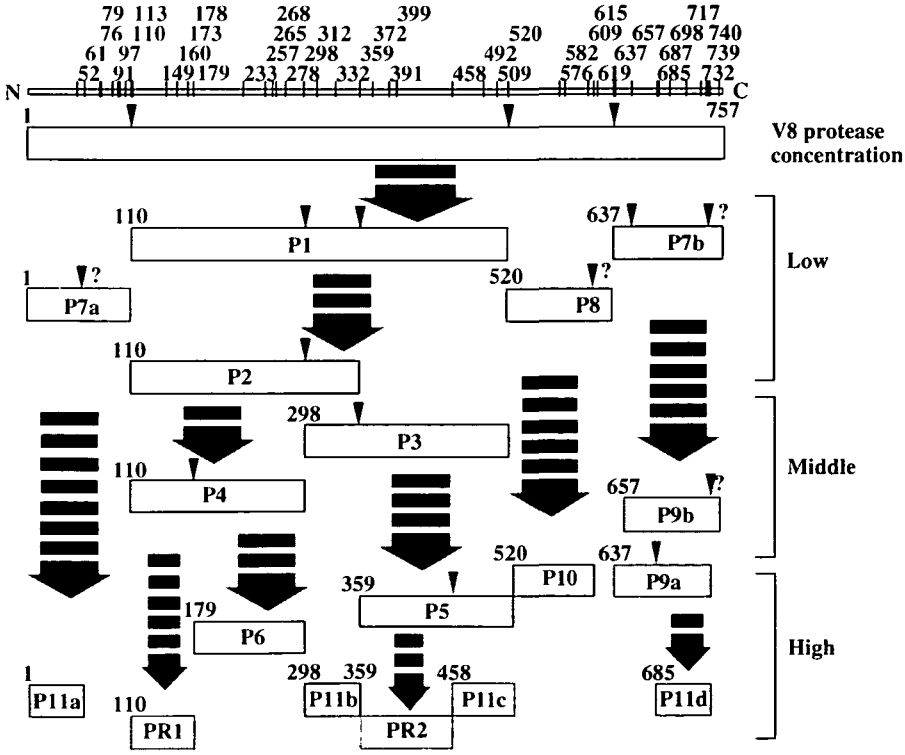

Fig. 3. **Cleavage order of the PB1 protein by V8 protease.** PB1 was treated with different concentrations of V8 protease and the order of cleavage was determined by measuring the appearance of each cleavage fragment. The decreasing width of arrows represents the increasing concentrations of V8 protease used. The amino acid sequence was determined for the amino-terminal region of all the fragments shown (see Table I), and the number of amino-terminal residue as counted from the amino terminus of intact PB1 is indicated at left side of each fragment. All the potential cleavage sites of PB1 by V8 protease are indicated on the top of intact PB1 protein.

size. Both P9 and P11 showed diffuse bands, suggesting that these two bands were mixtures of peptides of similar sizes.

Each of these peptides was transferred from the gel onto a PVDF membrane and analyzed for at least 10 amino acids from the amino terminus (Table I). The results indicated that the sequences of all these peptides perfectly matched with different parts of the PB1 protein. After sequence analysis, we confirmed that both band P9 and P11 were mixtures of different peptides, and we found that band P7 also contained two fragments of similar sizes. These peptides were renamed in alphabetical order as P7a/P7b, P9a/P9b, and P11a/P11b/P11c/P11d, respectively. In the P11 mixture, the relative contents of two components, P11c and P11d, were less than those of the other two components (see Table I). From the order of appearance with increase in the V8 protease concentration, the order of cleavage was estimated as summarized in Fig. 3.

Controlled proteolysis often generates domains that exist in intact proteins. Upon proteolysis of PB1, four fragments, P7a, P1, P8, and P7b, were produced at low doses of V8 protease (see Fig. 2), which correspond to one amino terminal domain (P7a; amino acid residues 1-109) for PA contact (*11*), two domains for RNA synthesis (P1 consisting of residues 110-519 plus P8 consisting of residues 520-636) containing all four RNA-dependent RNA polymerase motifs, and one carboxy-terminal domain (P7b; residues downstream from 637) for PB2 contact (*11*), respectively. Both of the terminal domains, P7a and P7b, are relatively resistant to further digestion by V8 protease, suggesting that each of these domains forms a single compact structural unit. Upon addition of high doses of V8 protease, the amino-terminal P7a fragment was cleaved to generate P11a, while the carboxy-terminal fragment P7b was cleaved to produce P11d *via* P9a/P9b intermediates. The amino terminal-proximal portion of the internal fragment P1 was cleaved into P2, which was further cleaved to generate P6 (*via* P4) and P11b (see Fig. 3). On the other hand, the carboxyl terminal portion of P1 was cleaved *via* P3 to p11c and P5 (see Fig. 3). Since the amino-terminal portion of P4 and that of P5 were identified in none of the bands analyzed, we isolated P4 and P5 and treated them with V8 protease. As a result, we identified new fragments, PR1 and PR2, from P4 and P5, respectively (data not shown).

Identification of 8-N_3 GTP-Crosslinked Fragments—8-N_3 [α-^{32}P]GTP-crosslinked PB1 was mixed with excess amount of unlabeled PB1 and treated with various concentrations of V8 protease. As shown in Fig. 4, the radioactivity was detected for P1, P2, P3, P4, P5, P6, all derived from the internal part of PB1 polypeptide between amino acid

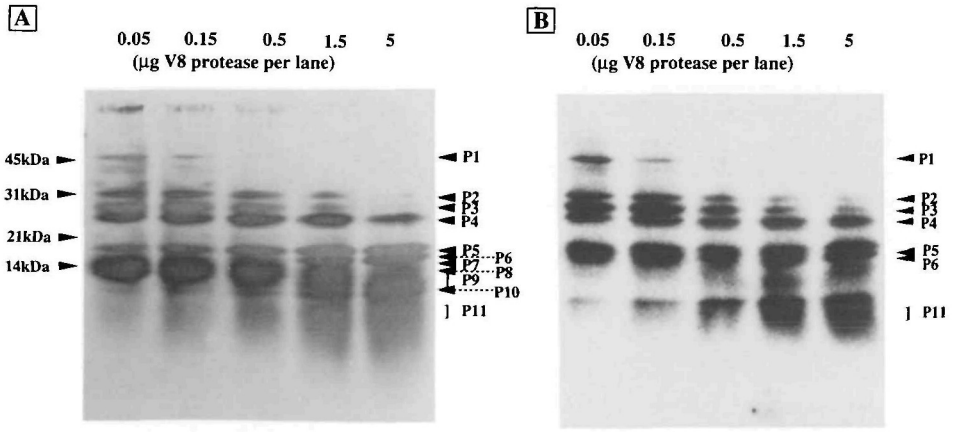

Fig. 4. **Digestion of the 8-N_3 GTP-crosslinked PB1 protein with V8 protease.** Isolated RNP was photo-crosslinked with 8-N_3 [α-^{32}P]GTP and the labeled PB1 was isolated by 0.1% SDS-7.5% PAGE. The gel slice containing the radio-labeled PB1 was mixed with unlabeled PB1 and the indicated amount of V8 protease. The mixtures were subjected onto 0.1% SDS-15% PAGE. V8 digestion was carried out for 8 h in the stacking gel (*8*). After electrophoresis, fragments were transferred onto a PVDF membrane and stained with Coomassie Brilliant Blue (A). The stained membrane was exposed to X-ray films for autoradiography (B). Migrating positions of the standard proteins are indicated on the left, while positions of the PB1 cleavage products are indicated on the right.

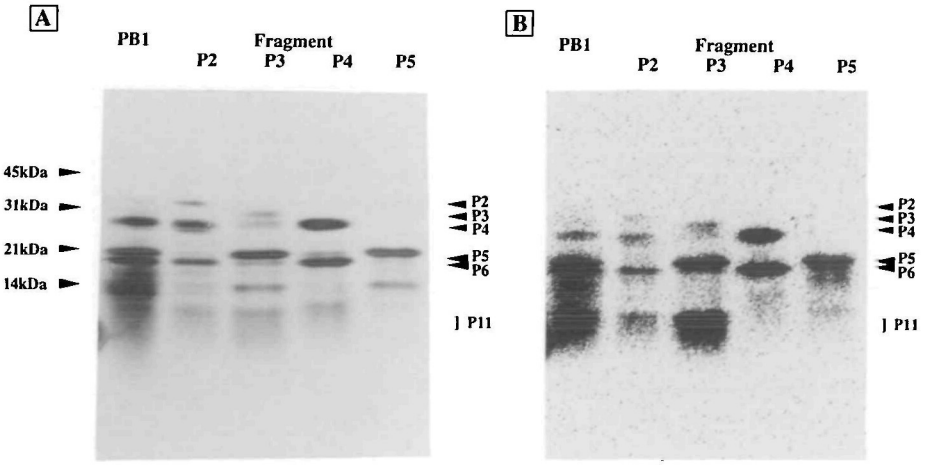

Fig. 5. **Secondary digestion of the 8-N_3 GTP-crosslinked PB1 fragments by V8 protease.** V8 fragments of the 8-N_3 GTP-crosslinked PB1 were isolated as in Fig. 4. The isolated fragments, P2, P3, P4, and P5, were subjected to the second cycle of V8 digestion. The peptides were transferred onto a PVDF membrane and stained with Coomassie Brilliant Blue R250 (A). The membrane was then exposed to X-ray films for autoradiography (B). Positions of the standard proteins are indicated on the left, while positions of the cleavage products are indicated on the right.

residue 110 and 519, and P11 band, which includes four small peptides (see Table I). In order to identify the 8-N_3 GTP-crosslinked fragment precisely, we isolated each of the labeled fragments and subjected them to the second cycle of V8 treatment. Figure 5A shows the stained gel pattern after SDS-PAGE, while Fig. 5B shows an autoradiogram of the gel. From the stained pattern (Fig. 5A) and the proteolytic cleavage map (see Fig. 3), we estimated that: P2 generated P4, P6, PR1, and P11b; P3 generated P5, PR2, P11b, and P11c; P4 generated P6 and PR1; and P5 generated PR2 and P11c. In addition, an as yet unidentified band of about 14 kDa was identified for the V8 digests of isolated P3 and P5, suggesting the presence of another intermediate between P3/P5 and PR2/P11c. As shown in Fig. 5B, the radioactivity was detected for P4, P6 and P11b (lane P2), P5 and P11b (lane P3), and P6 (lane P4). Since the digestion of the labeled P5 was incomplete (Fig. 5B, lane P5), we repeated the experiment for P5 and found that the radioactivity was quantitatively converted into P11c band, but not PR2 (data not shown).

The results together indicate that 8-N_3 GTP was crosslinked to three non-overlapping fragments, P6 (residue 179 to 297), P11b (residue 298 to 358), and P11c (residue 458 to 519). From the location of these three fragments, it is most likely that there are two GTP-binding sites on PB: the two adjacent fragments, P6 (residue 179 to 297) and P11b (residue 298 to 358), form the amino terminal-proximal GTP-binding site, designated as the GTP-binding site I; and P11c (residue 458 to 519) forms the carboxy terminal-proximal GTP-binding site II. GTP-binding site II on the fragment P11c is separated from the site I, presumably located at the boundary between P6 and P11b fragments. The highest labeling of radioactive 8-N_3 GTP was observed for fragment P11b (residue 298 to 358), and a smaller amount of radioactivity was associated with P6 (residue 179 to 297) and P11c (residue 458 to 519).

Identification of Dialdehyde GTP-Crosslinked Fragments—The binding site of oxidized GTP was also examined by proteolytic cleavage of the PB1 protein crosslinked with radioactive dialdehyde GTP. Radioactivity was found to be associated at least with seven proteolytic fragments, P1, P2, P3, P4, P5, P6, and P11 (Fig. 6). These labeled fragments were completely identical with those derived from the azido GTP-crosslinked PB1 (see Figs. 4 and 5). P1, P2, and P4 are all intermediate fragments in the generation of P6 (see Fig. 3), while P3 and P5 are converted to P11b and P11c (see Fig. 3), supporting the previous conclusion that there are two GTP-binding sites on PB1, site I between Met179 and Glu358, and site II between Gly458 and Glu519. However, the relative levels of radioactivity of three non-overlapping fragments, P6, P11b, and P11c, were 59, 28, and 15%, respectively, which are different from that of 8-N_3 GTP-crosslinked PB1. The level of crosslinking of oxidized GTP to fragment P6, the amino terminal half of site I, was about twice the level of azido GTP, while the crosslinked level of oxidized GTP to P11b, the carboxy terminal half of the site I, was about half the level of azido GTP crosslinking. This may suggest that the ribose moiety of GTP bound in site I faces the amino terminal proximal half, while the guanine moiety is associated with the carboxy terminal half.

Possible Roles of Two GTP-Binding Sites—Influenza virus RNA polymerase utilizes capped RNA as primers for transcription. This requirement can be bypassed by adding high concentrations of di- or trinucleotides. Among various combinations of dinucleotides, ApG is the best primer presumably because it is complementary to the 3′-terminal sequences of vRNA (*19*). In order to test the possibility that one of the two GTP-binding sites represents the primer-binding site, we examined the effect of ApG addition on the 8-N_3 GTP binding to the two sites. At 1 mM ApG, the total amount of radioactive GTP binding to PB1 was reduced to 60% (data not shown). The inhibition of GTP

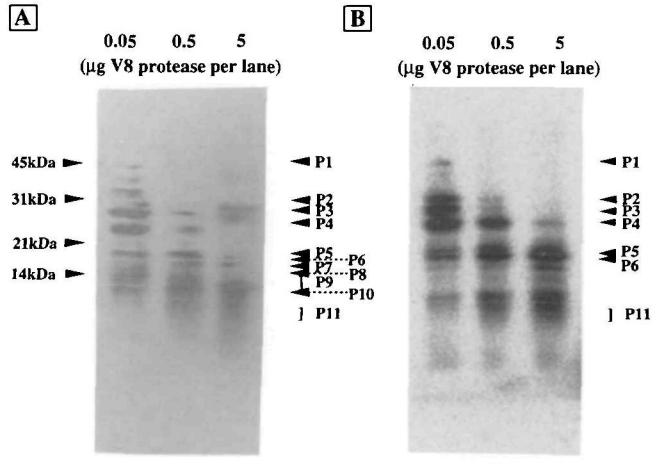

Fig. 6. **Digestion of the oxidized GTP-crosslinked PB1 protein with V8 protease.** Isolated RNP was crosslinked with oxidized [α-^{32}P]GTP and the labeled PB1 was isolated by 0.1% SDS-7.5% PAGE. The gel slice containing the radio-labeled PB1 was mixed with unlabeled PB1 and the indicated amount of V8 protease. The mixtures were subjected onto 0.1% SDS-15% PAGE. V8 digestion was carried out for 8 h in the stacking gel (*8*). After electrophoresis, fragments were transferred onto a Pro-Blot membrane and stained with Coomassie Brilliant Blue R250 (A). The stained membrane was exposed to X-ray films for autoradiography (B). Migrating positions of the standard proteins are indicated on the left, while positions of the cleavage products are indicated on the right.

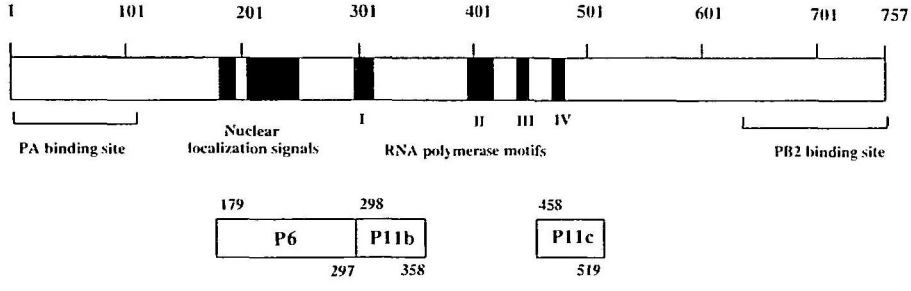

Fig. 7. **Functional map of the PB1 protein.** PB1 of influenza virus A/PR8/34 is composed of 757 amino acid residues. The subunit-subunit contact with PA is located at its amino terminal-proximal region while that with PB2 is at the carboxy terminal region (*23*). The four conserved motifs among RNA-dependent RNA polymerases are located in the middle portion of PB1. GTP analogues were crosslinked to three fragments, P6, P11b, and P11c.

binding to P5, P6, and P11c fragments was 58, 49, and 68%, respectively. One possible explanation for the differential inhibition of GTP binding by ApG is that GTP-binding site I at the boundary between P6 and P11b is the site of primer binding, and site II located within P11c fragment is for substrate binding.

DISCUSSION

Influenza virus RNA-dependent RNA polymerase is a unique multifunctional enzyme consisting of multiple subunits and carrying various activities required for transcription and replication. The concept that the PB1 subunit is not only the core subunit in function with the catalytic activity for RNA polymerization but also the core subunit in structure for assembly of other two subunits, PB2 and PA, was supported by several independent observations: (i) model RNA template-directed RNA synthesis *in vitro* was detected in extracts of cells expressing only PB1 after infection of recombinant baculovirus (*20*) or vaccinia virus (*21*) both carrying a cDNA for PB1 protein; (ii) a transfected model RNA template can be transcribed in cells expressing only the PB1 protein without PB2 and PA (*14*); (iii) any mutation in the four conserved motifs of PB1 renders the RNA polymerase nonfunctional to various extents (*22*); (iv) PB1-PB2 and PB1-PA binary complexes are formed, but no complex is formed between PB2 and PA (*23*); and a substrate analogue, 8-N_3 GTP, can be photo-crosslinked only to PB1 subunit (*8*). Here we confirmed the binding of GTP to PB1 alone using crosslinking of an oxidized GTP with aldehyde at the ribose moiety.

Controlled proteolysis often provides evidence of the overall scheme of domain organization of proteins. In the present study, we employed V8 protease treatment for the domain mapping for the PB1 protein of influenza virus RNA polymerase. The results described here indicate that PB1 is composed of four domains, two terminal domains (the amino-terminal fragment P7a from residue 1 to 109, and the carboxy-terminal fragment P7b from residue 637 to 757) and two internal domains (fragment P1 from residue 110 to 519, and fragment P8 from residue 520 to 636), which are generated by V8 treatment under mild conditions. The amino-terminal domain P7a and the carboxy-terminal domain P7b correspond to the subunit-subunit contact domain with PA and PB2, respectively (*23*). Co-transfection of pairs of P proteins and immuno-precipitation of P complexes indicate that binary complexes are formed between PB1 and PB2, and between PB1 and PA, but not between PB2 and PA, indicating that PB1 is the core subunit in the assembly of three different subunits. Furthermore, using a nested set of deletion mutants for each P protein, we found that PA binds to the amino-terminal region of PB1 upstream from residue 100, while PB2 binds to the carboxy-terminal region of less than 100 amino acid residues in length (*23*; Djanybek, A. and Ishihama, A., unpublished), implying that both terminal domains may not be involved in the catalytic function of RNA polymerase. In concert with these results of subunit-subunit contact site mapping on PB1, 8-N_3 GTP was selectively crosslinked to P1, one of the two initial cleavage products derived from the internal region of PB1. Thus, we conclude that the P1 domain corresponds to the catalytic domain of RNA polymerization. The presence of all four consensus motifs of RNA-dependent RNA polymerase (*24*) in the P1 fragment of influenza virus PB1 protein also supports the prediction that this region is responsible for RNA polymerization.

PB2 carries the binding site for capped RNA and the endonucleolytic cleavage site of capped RNA (*25-29*). The domain in PB2 carrying the binding site of capped RNA has also been identified by the same procedure as employed in this study (Honda, A. and Ishihama, A., in preparation). However, it remains unsolved how the capped RNA primer generated by the PB2 subunit is transferred from the endonucleolytic cleavage site on PB2 to the PB1 subunit with the catalytic function of RNA synthesis. Knowledge of the structural organization between two subunits is crucial to understand the functional coordination between these two subunits each carrying multiple and different functions. The domain (P8) of PB1 connecting the catalytic domain (P1) and the PB2-contact domain (P7b) may play a key role in this process.

Crosslinking studies of nucleotides have contributed much to our understanding of the catalytic pockets of DNA and RNA polymerases. Our crosslinking experiments using both 8-N_3 GTP and oxidized GTP indicated that there are two GTP-binding sites within the P1 domain, both derived from the middle part of PB1 protein. GTP-binding site I is located near residue 297/298 at the boundary between P6 and P11b fragments (Fig. 7). The oxidized GTP can be crosslinked to protein Lys residues (*15*). The P6 fragment carries 14 Lys residues at position 188, 197, 198, 207, 209, 214, 229, 235, 237, 265, 278, 279, 281, and 288, while the P11b fragment contains 3 Lys residues at position 308, 347, and 353. The identification of the specific Lys residue(s) crosslinked with the GTP analogue remains to be determined. Since the motif 1 of RNA-dependent RNA polymerase is located at the same region, being split into the carboxy-terminus of P6 and the amino-terminus of P11c, we tentatively propose that the motif 1 is related to this GTP-binding activity. Since the inhibition of GTP binding to site I by ApG, the artificial primer commonly used for transcription initiation *in vitro* in place of capped RNA (*19*), is more than that to site II, one possibility is that site I is the primer-binding site of influenza virus RNA polymerase. If this is the case, the cleavage products of capped RNA generated on PB2 must be transferred onto this site of PB1 prior to functioning as primers. The primer-binding site should also function as the binding site of nascent RNA chains.

From the three-dimensional structures of HIV-1 reverse transcriptase, phage T7 RNA polymerase, and Klenow fragment of *E. coli* DNA polymerase I, the conserved motifs 1 and 3 are considered to form the catalytic domain, in which an Asp residue in motif 1 and Asp-Asp dipeptide in motif 3 are involved in the catalytic pocket (*30*). In the case of influenza virus PB1 protein, these Asp residues correspond to Asp305 in motif 1 and Asp445 and Asp446 in motif 3. Recently, a crosslinking study of oxidized nucleoside triphosphates was carried out for polio virus RNA polymerase (*31*), which suggested the presence of two NTP-binding sites, one within the motif 3 but the other near the amino terminus with as yet no known function.

GTP-binding site II of the PB1 subunit of influenza virus RNA polymerase is, however, located within fragment P11c between residue 458 and 519, including the conserved motif 4 of RNA-dependent RNA polymerases (Fig. 7). This

is the first finding that indicates the presence of nucleotide-binding site within the motif 4. The P11c fragment contains 4 Lys residues at position 471, 479, 480, and 481, among which Lys481 is included in the motif 4. The possibility that the GTP-binding site II represents the substrate-binding site of viral RNA polymerase remains to be determined.

REFERENCES

1. Ishihama, A. and Nagata, K. (1988) Viral RNA polymerase. *CRC Crit. Rev. Biochem.* **23**, 27-76
2. Krug, R.M., Alonso-Caplen, F.V., Julkunen, I., and Katze, M.G. (1989) Expression and replication of the influenza virus genome in *The Influenza Viruses* (Krug, R.M., ed.) pp. 89-152, Plenum Press, New York
3. Ishihama, A. and Barbier, P. (1994) Molecular anatomy of viral RNA-directed RNA polymerases. *Arch. Virol.* **134**, 235-258
4. Honda, A., Mukaigawa, J., Yokoiyama, A., Kato, A., Ueda, S., Nagata, K., Krystal, M., Nayak, D.P., and Ishihama, A. (1990) Purification and molecular structure of RNA polymerase from influenza virus A/PR8. *J. Biochem.* **107**, 624-628
5. Ulmanen, I., Broni, B.A., and Krug, R.M. (1981) Role of two of the influenza virus core P proteins in recognizing cap 1 structures (m7GpppNm) on RNAs and in initiating viral RNA transcription. *Proc. Natl. Acad. Sci. USA* **78**, 7355-7359
6. Blaas, D., Patzelt, E., and Kuechler, E. (1982) Identification of the cap binding protein of influenza virus. *Nucleic Acids Res.* **10**, 4803-4812
7. Ulmanen, I., Broni, B., and Krug, R.M. (1983) Influenza virus temperature-sensitive cap (m7GpppNm)-dependent endonuclease. *J. Virol.* **45**, 27-35
8. Asano, Y., Mizumoto, K., Maruyama, T., and Ishihama, A. (1995) Photoaffinity labeling of influenza virus RNA polymerase PB1 subunit with 8-azido GTP. *J. Biochem.* **117**, 677-682
9. Braam, J., Ulmanen, I., and Krug, R.M. (1983) Molecular model of a eucaryotic transcription complex: functions and movements of influenza P proteins during capped RNA-primed transcription. *Cell* **34**, 609-618
10. Fodor, E., Seong, B.L., and Brownlee, G.G. (1993) Photochemical cross-linking of influenza A polymerase to its virion RNA promoter defines a polymerase binding site at residues 9 to 12 of the promoter. *J. Gen. Virol.* **74**, 1327-1333
11. Toyoda, T., Adyshev, D., Kobayashi, M., Iwata, A., and Ishihama, A. (1996) Molecular assembly of influenza virus RNA polymerase: Identification of the subunit-subunit contact sites on each P protein subunit. *J. Gen. Virol.* **77**, 2149-2157
12. Krug, R.M., Ueda, M., and Palese, P. (1975) Temperature-sensitive mutants of influenza WSN virus defective in virus-specific RNA synthesis. *J. Virol.* **16**, 790-796
13. Mahy, B.W.J., Barrett, T., Nichol, S.T., Penn, C.R., and Wolstenholme, A.J. (1981) Analysis of the function of influenza virus genome RNA segments by use of temperature-sensitive mutants of fowl plaque virus in *The Replication of Negative Strand Viruses* (Bishop, D.H.L. and Compans, R.W., eds.) pp. 379-387, Elsevier, New York
14. Nakagawa, Y., Oda, K., and Nakada, S. (1996) The PB1 subunit alone can catalyze cRNA synthesis, and the PA subunit in addition to the PB1 subunit is required for viral RNA synthesis in replication of the influenza virus genome. *J. Virol.* **70**, 6390-6394
15. Clertant, P. and Cuzin, F. (1982) Covalent affinity labeling by periodate-oxidized [α-^{32}P]ATP of the large-T proteins of polyoma and SV40 viruses. *J. Biol. Chem.* **257**, 6300-6305
16. Young, J.F., Desselberger, U., Graves, U., Palese, P., Shatzman, A., and Rosenburg, M. (1983) Cloning and expression of influenza virus genes in *The Origin of Pandemic Influenza Viruses* (Laver, W.G., ed.) pp. 129-138, Elsevier, New York
17. Studier, F.W., Rosenberg, A.H., Dunn, J.J., and Dubendorff, J. W. (1990) Use of T7 RNA polymerase to direct expression of cloned genes. *Methods Enzymol.* **185**, 60-89
18. Kobayashi, M., Tuchiya, K., Nagata, K., and Ishihama, A. (1992) Reconstitution of influenza virus RNA polymerase from three subunits expressed using recombinant baculovirus system. *Virus Res.* **22**, 235-245
19. Honda, A., Mizumoto, K., and Ishihama, A. (1986) RNA polymerase of influenza virus. VII. Dinucleotide-primed initiation of transcription at specific sites on viral RNA. *J. Biol. Chem.* **261**, 5987-5991
20. Kobayashi, M., Toyoda, T., and Ishihama, A. (1996) Influenza virus PB1 protein is the minimal and essential subunit of RNA polymerase. *Arch. Virol.* **141**, 525-533
21. Toyoda, T., Kobayashi, M., Nakada, S., and Ishihama, A. (1996) Molecular dissection of influenza virus RNA polymerase: PB1 subunit alone is able to catalyze RNA synthesis. *Virus Genes* **12**, 155-161
22. Biswas, S.K. and Nayak, D.P. (1994) Mutational analysis of the conserved motifs of influenza A virus polymerase basic protein 1. *J. Virol.* **68**, 1819-1826
23. Toyoda, T., Adyshev, D.M., Kobayashi, M., Iwata, A., and Ishihama, A. (1996) Molecular assembly of influenza virus RNA polymerase: Identification of the subunit-subunit contact sites on each P protein subunit. *J. Gen. Virol.* **77**, 2149-2157
24. Poch, O., Sauvaget, I., Delarue, M., and Tordo, N. (1990) Identification of four conserved motifs among the RNA-dependent polymerase encoding elements. *EMBO J.* **8**, 3867-3874
25. Ulmanen, I., Broni, B.A., and Krug, R.M. (1983) Influenza virus temperature-sensitive cap (m^{7}GpppNm)-dependent endonuclease. *J. Virol.* **45**, 27-35
26. Mandler, J., Muller, K., and Scholtissek, C. (1991) Mutants and revertants of an avian influenza A virus with temperature-sensitive defects in the nucleoprotein and PB2. *Virology* **181**, 512-519
27. Licheng, S., Summers, D.F., Peng, Q., and Galarza, J.M. (1995) Influenza A virus polymerase subunit PB2 is the endonuclease which cleaves host cell mRNA and functions only as the trimeric enzyme. *Virology* **208**, 38-47
28. Nakagawa, Y., Kimura, N., Toyoda, T., Mizumoto, K., Ishihama, A., Oda, K., and Nakada, S. (1995) The RNA polymerase PB2 subunit is not required for replication of the influenza virus genome but is involved in capped mRNA synthesis. *J. Virol.* **69**, 728-733
29. Shi, L.C., Summers, D.F., Peng, Q.H., and Galarza, J.M. (1995) Influenza A virus RNA polymerase subunit PB2 is the endonuclease which cleaves host cell mRNA and functions only as the trimeric enzyme. *Virology* **208**, 38-47
30. McAllister, W.T. and Raskin, C.A. (1993) The phage RNA polymerase are related to DNA polymerases and reverse transcriptases. *Mol. Microbiol.* **10**, 1-6
31. Richards, O.C., Hanson, J.L., Schultz, S., and Ehrenfeld, E. (1995) Identification of nucleotide binding sites in the poliovirus RNA polymerase. *Biochemistry* **34**, 6288-6295